Long-Term Oxidation of Superalloys*

C. L. Angerman†

The oxidation of 24 commercially available superalloys was measured after exposure in still air at up to 1150°C for up to 10,000 hr. The total depth affected by oxidation, which includes subscale reactions, followed the expected exponential relationship with temperature and the expected parabolic relationship with exposure time at 1000°C; oxidation of "Haynes" 25 and TD nickel chromium was not parabolic at 1150°C. The alloys could be divided into four groups according to relative resistance to oxidation at 1000°C. These differences in resistance could be explained qualitatively by the nominal compositions of the alloys.

INTRODUCTION

Because of their strength and resistance to oxidation at elevated temperatures, the nickel- and cobalt-based superalloys are candidate cladding for radio-isotope heat sources that could supply power for remote marine and terrestrial locations. The superalloys are particularly suited for encapsulating irradiated cobalt metal (^{60}Co) for these heat source applications.[1,2] Resistance to oxidation is required because heat source capsules may be directly exposed to a heat transfer fluid that contains oxygen or oxide compounds as impurities or to air under emergency conditions. Problems of compatibility between capsule materials and cobalt are minimized because the properties of the superalloys and cobalt are similar. Since no gas is generated inside the capsule as the ^{60}Co decays, the stress in the capsule wall is low (< 500 psi)

and makes feasible the desired service life of 1–5 years at temperatures near 1000°C. The service life is based on the half-life of ^{60}Co, 5.27 yr; high temperatures are required to increase the efficiency of the power conversion systems.

This report summarizes measurements of the oxidation of 24 super-alloys during exposure to still air at up to 1150°C for times as long as 10,000 hr. Published oxidation data were inadequate to predict the resistance of the superalloys to oxidation at the expected service conditions. These tests were part of a program to select suitable alloys for encapsulating ^{60}Co, define the limiting operating conditions, and demonstrate the performance of capsules at typical heat source conditions.[3–5]

EXPOSURE CONDITIONS

The 24 alloys that were tested are listed in Table I with their compositions and a summary of oxidation test results. Most of the alloys were selected because published oxidation data suggested that they might withstand the expected operating conditions of heat sources. Other alloys were selected because they were representative of certain classes of alloys. For example, "Tophet" A, "Tophet" C, and "Haynes" 150 are simple binary or ternary alloys based on nickel or cobalt; GE 2541 and "Haynes" 188 have minor additions of rare earth elements. Three commercial grades of pure nickel were selected as reference materials. Only a few iron-based alloys were tested because published data indicated that they would have an inadequate resistance to oxidation. None of the precipitation-hardenable alloys, such as "Udimet" 700 or IN-100, were tested because the phases responsible for the increased strengths of these alloys begin to dissolve at the expected service conditions.[20]

Since the purpose of these tests was to provide data for predicting the performance of the alloys, exposure conditions were designed to measure the kinetics of oxidation. The effect of temperature was measured by exposing cylindrical samples 0.250 to 0.500 inch in diameter × 0.500 inch long to still air (ambient muffle furnace atmosphere) for 500 hr at 850, 950, 1000, and 1150°C. The effect of time at temperature was measured by exposing coupons 1.000 in. long × 0.500 in. wide × 0.060 to 0.080 in. thick at 1000°C for 1000, 5000, and 10,000 hr. All samples were heated at each temperature concurrently in the same furnace. Cylindrical samples of the more resistant alloys were exposed for 3000 hr at 1150°C in an accelerated test to confirm the kinetics observed in the other tests. The latter conditions were selected because the expected amount of oxidation would be approximately the same as that predicted for typical operating conditions of a heat source, 50,000 hr at 1000°C.

Table I. Oxidation of Superalloys at 1000°C

| Alloy | Source | Nominal composition (wt. %) | | | | | | | | | | Zone thickness (mils) — 1000-hr Test | | | |
		Ni	Co	Fe	Cr	Mo	W	Mn	Si	C	Others	Surface scale	Intergranular penetration	Alloy depletion	Total[j]
Group A															
TD nickel chromium	Fansteel	78	—	—	20	—	—	—	—	0.05	ThO_2-2	<0.1	—	—	<0.1
Group B															
"Hastelloy" X	Union Carbide	49	1	18	22	9	—	0.5	0.5	0.10	—	0.6	1.7	—	2.3
"Haynes" 25	Union Carbide	10	50	3	20	—	15	1.5	1.0	0.10	—	0.7	3.6	3.6	4.3
GE 2541	General Electric	—	—	72	24	—	—	1.0	1.0	0.10	Al-4, Y-0.2	0.1	2.9	—	3.0
"Hastelloy" C	Union Carbide	57	—	5	15	16	4	1.0	1.0	0.08	—	1.0	2.0	—	3.0
"Tophet" C	W. B. Driver	59	—	23	16	—	—	1.0	0.7	0.15	—	0.4	2.7	—	3.1
"Inconel" 600	International Nickel	75	—	7	16	—	—	1.0	0.5	0.10	—	1.0	1.6	—	2.6
50 Ni–50 Cr	International Nickel	50	—	—	50	—	—	1.0	1.0	—	—	0.9	2.6	—	3.5
"Haynes" 188	Union Carbide	22	38	3	22	—	14	1.0	0.5	0.10	La-0.1	0.3	1.9	3.2	3.5
"Incoloy" 800	International Nickel	32	—	45	21	—	—	1.5	1.0	0.10	—	0.4	3.4	4.8	5.2
GE 1541	General Electric	—	—	80	15	—	—	—	—	—	Al-4, Y-0.8	0.1	2.3	—	2.4
Group C															
N-155	Carpenter Steel	20	20	31	21	3	2	1.5	0.5	0.15	Cb-1	0.8	2.0	4.4	5.2
"Incoloy" 825	International Nickel	42	—	29	22	3	—	1.0	0.5	0.05	Cu-2, Ti-1	1.4	1.6	5.1	4.5
"Inconel" 625	International Nickel	62	—	3	22	9	—	0.1	0.3	0.05	Cb-4	0.8	4.4	5.8	5.8
RA-333	Rolled Alloys	45	3	18	25	3	3	2.0	1.0	0.08	—	1.3	5.0	5.0	6.3
"Hastelloy" F	Union Carbide	41	2	24	22	6	1	1.5	1.0	0.05	Cb-2	1.6	3.0	—	4.6
"Tophet" A	W. B. Driver	78	—	1	20	—	—	0.1	1.5	0.1	—	0.4	5.0	—	5.4
"Tophet" 30	W. B. Driver	69	—	—	30	—	—	1.0	1.0	0.03	—	0.4	2.7	8.0	8.4
"Hastelloy" G	Union Carbide	48	—	19	22	6	—	1.3	0.3	0.03	Cb-2, Cu-2	1.5	4.0	—	5.5
"Haynes" 150	Union Carbide	—	50	21	28	—	—	0.5	0.7	0.1	—	1.4	6.0	—	7.4
Group D															
TD Nickel	Fansteel	98	—	—	—	—	—	—	—	—	ThO_2-2	10.8	—	—	10.8
Ni 270	International Nickel	99.9	—	—	—	—	—	—	—	0.02	—	11.0	—	—	11.0
Ni 201	International Nickel	99.5	—	—	—	—	—	—	0.3	0.02	—	14.6	—	—	14.6
Ni 200	International Nickel	99.5	—	—	—	—	—	—	0.3	0.15	—	16.8	—	—	16.8

Table I. Continued

Alloy	Source	5000-hr Test Surface scale[a]	Inter-granular penetration	Alloy depletion	Total	10,000-hr Test Surface scale[a]	Inter-granular penetration	Alloy depletion	Total	50,000 hr Extrap. total	Ref. number for Fig. 8
Group A											
TD nickel chromium	Fansteel	0.8	—	—	0.8	2.4	0	0	2.4[b]	4.0	1
Group 8											
"Hastelloy" X	Union Carbide	1.3	1.0	3.0	4.3	2.0	7.0	7.0	9.0[b]	18.0	2
"Haynes" 25	Union Carbide	2.0	4.0	4.0	6.0	2.0(2.0)	4.0	4.0	8.0	18.0	3
GE 2541	General Electric	0.4	2.8	—	3.2	0.5(5.0)	4.0	4.0	9.5	20.0	4
"Hastelloy" C	Union Carbide	1.8	3.2	6.2	8.0	3.0	3.0	8.0	11.0[b]	23.0	5
"Tophet" C	W. B. Driver	2.0	4.6	—	6.6	1.0(7.0)	4.0	4.0	12.0	25.0	6
"Inconel" 600	International Nickel	1.8	7.6	—	9.4	2.0	9.0	—	11.0[b]	26.0	7
50 Ni–50 Cr	International Nickel	1.4	—	5.0	6.4	2.0	7.0	16.0	18.0	27.0	8
"Haynes" 188	Union Carbide	3.0	3.0	9.0	12.0	1.5(4.0)	5.0	7.0	12.5	27.0	9
"Incoloy" 800	International Nickel	0.8	6.1	8.4	9.2	3.1	8.8	8.8	11.9[b]	28.0	10
GE 1541	General Electric	Not tested				Not tested				—	—
Group C											
N-155	Carpenter Steel	2.4	5.6	10.6	13.0	2.0(3.0)	5.0	8.0	13.0	35.0	11
"Incoloy" 825	International Nickel	3.0	9.0	9.0	12.0	4.0	13.0	13.0	17.0[b]	36.0	12
"Inconel" 625	International Nickel	4.0	6.0	9.3	13.3	0.5(3.0)	6.7	12.5	16.0[b]	37.0	13
RA-333	Rolled Alloys	1.0	2.0	6.0	7.0	6.0	8.0	10.0	16.0	37.0	14
"Hastelloy" F	Union Carbide	0.5(3.0)	4.0	5.0	8.5	2.0(3.0)	6.0	15.0	20.0	43.0	15
"Tophet" A	W. B. Driver	1.0	4.0	13.0	14.0	2.0(8.0)	6.0	10.0	20.0	43.0	16
"Tophet" 30	W. B. Driver	2.0	4.6	13.0	15.0	4.0(2.0)	6.0	10.0	16.0	45.0	17
"Hastelloy" G	Union Carbide	4.4	11.4	11.4	15.8	3.0(2.0)	7.0	16.0	21.0	48.0	18
"Haynes" 150	Union Carbide	Not tested				Not tested				—	—
Group D											
TD nickel	Fansteel	23.0	—	—	23.0	34.0	—	—	34.0[b]	75	19
Ni 270	International Nickel	26.7	—	—	26.7	36.0	20.0[c]	—	56.0[c]	>80	20
Ni 201	International Nickel	34.6	—	—	34.6	44.0	8.0[d]	—	52.0[d]	>100	21
Ni 200	International Nickel	41.3	8.0[d]	—	49.3[d]	e	—	—	e	>100	22

[a] Number in parentheses is thickness of scale that spalled.
[b] Test duration was 9400 hr instead of 10,000 hr.
[c] Remaining 20.0 mils intergranularly oxidized.
[d] Remaining 7.6 mils internally oxidized.
[e] Whole specimen converted to oxide.
[f] Total is surface scale plus maximum of either intergranular or alloy depletion.

EXAMINATION PROCEDURES

Capsules made from these materials must reliably contain the cobalt source under a wide variety of circumstances. Consequently, the measure of oxidation resistance most important to this application is the total depth affected by the various reactions that occur during oxidation. These reactions include formation of the surface scale, spalling of the scale, intergranular oxidation, internal oxidation, and depletion of the alloying constituents by diffusion to the sample surface where they become part of the oxide scale. In these tests the thickness of each of the reaction zones was measured on photographs at 100 to 250 × from at least three representative areas from the center of each sample. Loss of the surface scale by spalling was calculated from measurements of sample thickness, excluding the retained scale, before and after the test. The total depth affected by oxidation was the sum of the scale thickness, after correcting for any spalling, and the maximum depth in the metal affected by the surface reaction, whether caused by depletion of alloy constituents, internal oxidation, or grain boundary oxidation. (See Fig. 4 for examples.) Weight changes were measured on a few samples as an independent measure of scale spalling. The total depths affected were not corrected for the lower density of the oxide scale because the correction would be small for all the alloys.

X-ray diffraction and electron microprobe analyses were used to determine the compositions of the oxide scale and the alloy depletion zone and to identify the precipitates formed in the center of the samples as a result of long-term heating.

OXIDATION KINETICS

Effect of Temperature

The total depth affected by oxidation after 500 hr exposure increased with increasing temperature according to the expected exponential relationship (Table II and Fig. 1). The slopes of these curves correspond to "activation energies" between 24 and 37 kcal/mole, but the diffusional processes responsible for oxidation are too complex to attach any particular significance to these energy values.

The temperature dependence of oxidation in these tests is in general agreement with data of other investigators, as shown in Fig. 2. Although the slopes of the lines in Fig. 2 are nearly equal, the depths affected by oxidation were different. These differences are attributed to differences in test conditions and differences in the details of the measurements made in the various investigations. For example, scale thickness often was measured

Table II. Oxidation of Superalloys in 500-hr Tests

	"Inconel" 600	"Haynes" 25	"Hastelloy" C	"Hastelloy" X	TD Ni	TD Nickel chromium	"Incoloy" 825
	Thickness of affected zone (mils)						
850°C							
Surface scale	0.1	0.2	0.2	0.3	2.5	0.1	0.3
Intergranular penetration	0.4	0.3	<0.1	0.6	—	—	0.8
Alloy depletion	0.7	0.3	0.4	0.8	—	—	2.0
Total[c]	0.8	0.5	0.6	1.1	2.5	0.1	2.3
950°C							
Surface scale	0.7	0.4	0.5	0.5	6.5	0.2	1.0
Intergranular penetration	1.4	0.8	0.7	1.5	0.2[a]	—	2.3
Alloy depletion	2.1	1.5	0.8	2.5	—	—	4.0
Total	2.8	1.9	1.3	3.0	6.7	0.2	5.0
1000°C							
Surface scale	0.4	1.0	1.0	0.8	7.0	0.25[b]	—
Intergranular penetration	3.0	1.0	0.5	1.5	2.0[a]	—	—
Alloy depletion	3.0	2.2	2.5	4.0	—	—	—
Total	3.4	3.2	3.5	4.8	9.0	0.25	—
1150°C							
Surface scale	—	1.6	1.5	2.0	21.5	0.8	—
Intergranular penetration	—	1.5	3.5	4.5	—	—	—
Alloy depletion	—	3.0	10.0	7.5	—	—	—
Total	—	4.6	11.5	9.5	21.5	0.8	—

[a] Internal oxidation.
[b] Nonuniform; zone 8.0 mils thick in some areas, see text.
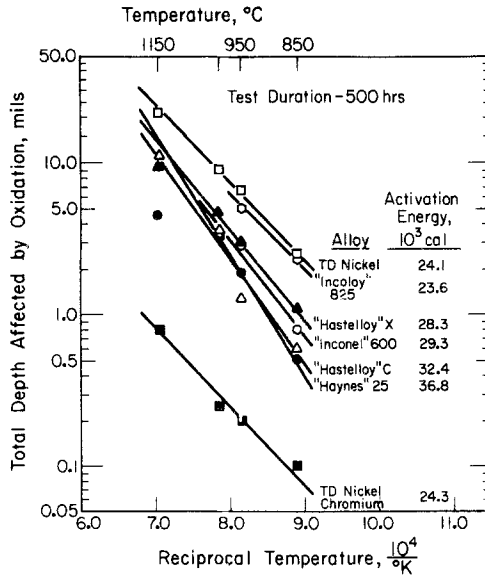[c] Total is surface scale plus maximum of either intergranular penetration or alloy depletion.

Fig. 1. Effect of temperature on oxidation.

in terms of weight change, or no measurements were made of the thickness of the alloy depletion zone.

Effect of Time

The total depth affected by oxidation increased with increasing time according to the expected parabolic relationship, although there was some scatter in the data (Table I and Fig. 3). Each reaction zone (surface scale, intergranular penetration, and alloy depletion) also grew parabolically with time as expected, indicating that the reactions were controlled by diffusion. The data for total thickness were extrapolated to 50,000 hr to select the best capsule alloys for further testing, and as indicated in Table I, the alloys could be ranked into four groups according to relative resistance to oxidation. The microstructure of the oxidation zone on a representative alloy from each group is shown in Fig. 4. Independent tests with selected alloys yielded identical results.[4]

Accelerated Tests

Cylindrical specimens of "Hastelloy" C, "Hastelloy" X, "Inconel" 600, "Haynes" 25, and TD nickel chromium were tested (3000 hr at 1150°C)
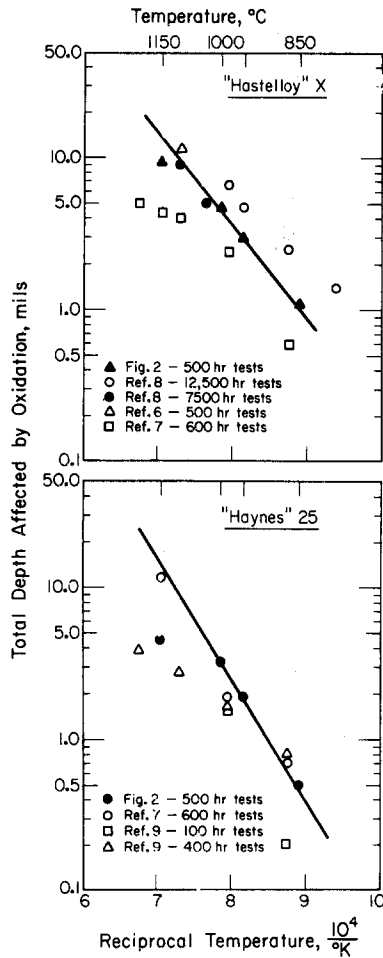
Fig. 2. Published data on oxidation of
"Hastelloy" X and "Haynes" 25.

to measure the ability to predict alloy performance from the kinetics observed
in the other tests. Good agreement between the observed and predicted
amounts of oxidation were obtained with the two "Hastelloys" and with
"Inconel" 600 (Table III). However, much higher than expected rates of
oxidation were observed over the entire surface of the "Haynes" 25 sample
and in one area of the TD nickel chromium sample.

A surface scale approximately four times thicker than predicted formed
on the "Haynes" 25 (Fig. 5). Wlodek[10] observed catastrophic oxidation
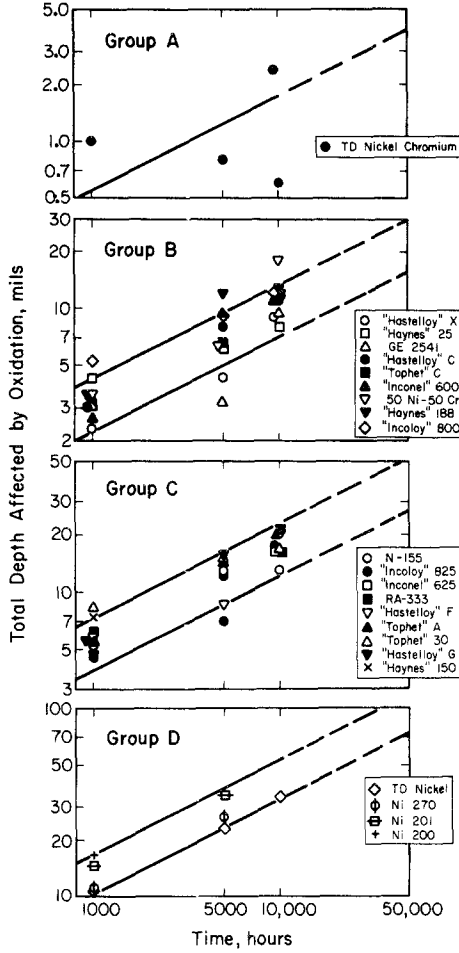
Fig. 3. Effect of time on oxidation at 1000°C.

at 1200°C and attributed the increased oxidation rate to the formation of a low melting scale containing a tungsten compound. Wolf and Sandrock[11] observed variations in the oxidation rate and indicated that the time–temperature thresholds for the catastrophic oxidation were related to the manganese and silicon contents of the particular heat of metal being tested.

Although the general oxidation of TD nickel chromium was about as predicted, a tenfold increase was measured in one region of the specimen (Fig. 6). This local attack occurred by the formation of a subsurface layer of oxide followed by intergranular penetration of the oxide along those
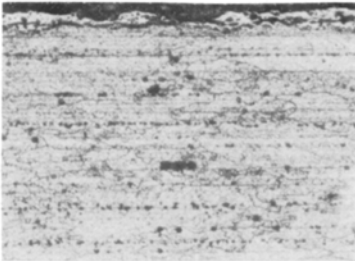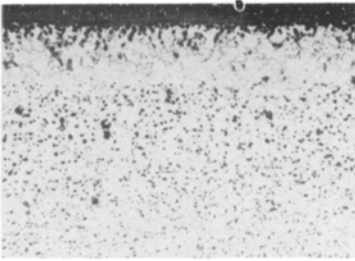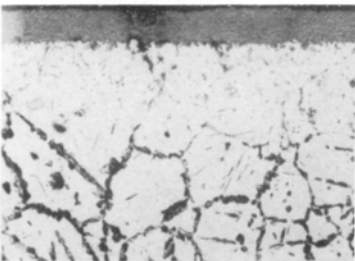
MATERIAL	TYPE OF REACTION	THICK. (mils)
Group A – TD Nickel Chromium		
	Oxide Scale	2.4
	Total Depth Affected	2.4
Group B – "Hastelloy" C		
	Oxide Scale	3.0
	Alloy Depletion	8.0
	Total Depth Affected	11.0
Group C – "Tophet" 30		
	Oxide Scale (Spalled Scale)	4.0 (2.0)
	Alloy Depletion	10.0
	Total Depth Affected	16.0
Group D – Nickel 201		
	Oxide Scale – two distinct layers	44.0
	Internal Oxidation	8.0
	Total Depth Affected	52.0

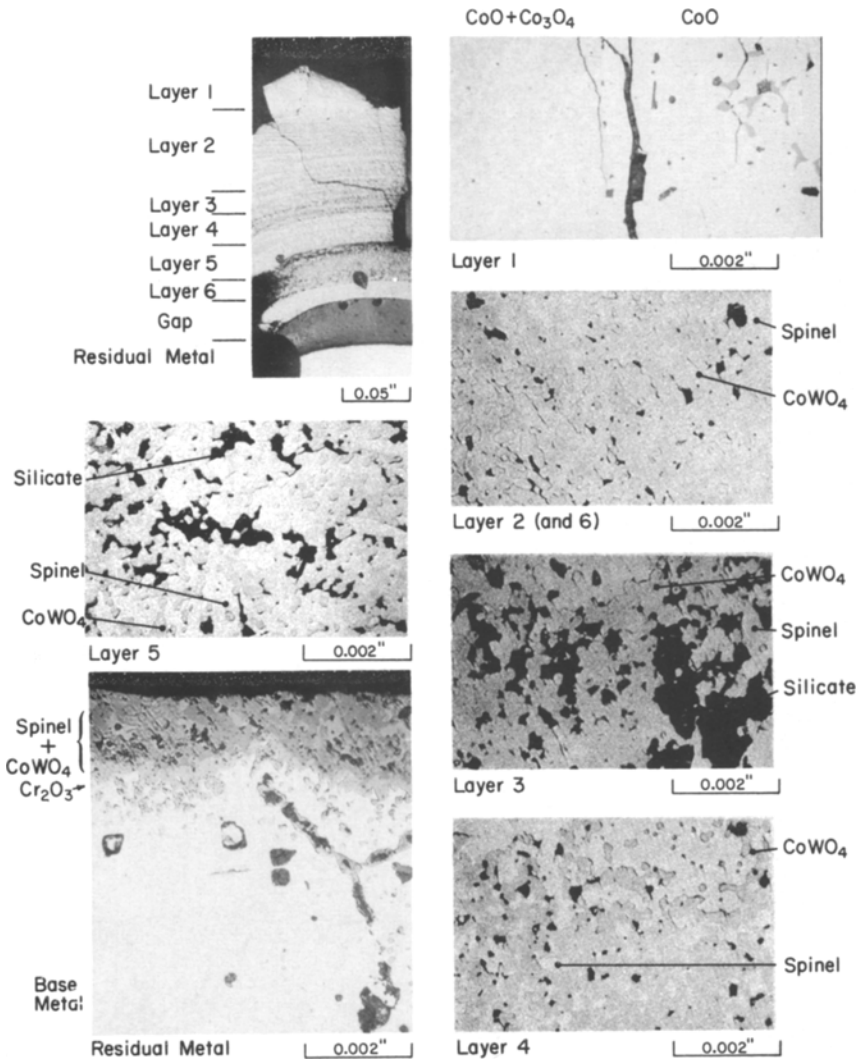**Fig. 4.** Typical oxidation after 10,000 hr at 1000°C.

Fig. 5. Multilayered oxide scale on "Haynes" 25 after 3000 hr at 1150°C.

grain boundaries that were depleted in thoria particles, presumably during the oxidation test. The "depleted" boundaries did not extend into the center of the specimen and did not occur in other regions of the specimen where oxidation was limited to the formation of a thin, continuous scale typical of that in other tests at less severe conditions. Such behavior was not reported in recent studies of the oxidation of other nickel–chromium–ThO_2 alloys.[12,13]

Table III. Results of Accelerated Oxidation Test in Still Air at 1150°C for 3000 hr

	Total depth affected by oxidation (mils)	
	Observed	Predicted
"Hastelloy" X	18.0	19.0
"Hastelloy" C	20.5	25.0
"Inconel" 600	38.5	49.0
TD Nickel chromium	(40)[a]	5.0
"Haynes" 25	175	41.5

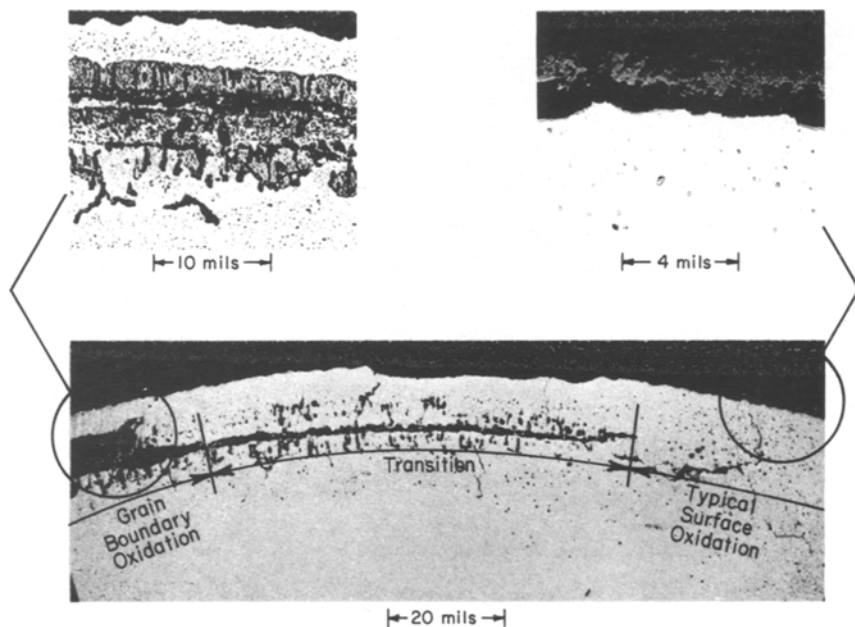[a] 40 mils in local area; 4 mils generally.

Fig. 6. Oxidation of TD nickel chromium after 3000 hr in still air at 1150°C.

OXIDE SCALE COMPOSITION

To aid in understanding the test results and assist in extrapolating them to longer times, the oxidized surfaces of selected samples of "Inconel" 600, "Hastelloy" C, "Hastelloy" X, "Haynes" 25, and TD nickel chromium were

analyzed by electron microprobe and x-ray diffraction techniques. The formation of relatively volatile oxides of alloy constituents, such as molybdenum and tungsten, could change the rates of oxidation. The microprobe analyses were made on the same samples as used for the metallographic measurements of oxide thickness. Because of the small amounts of oxide present on most samples, the x-ray diffraction patterns were taken directly from the oxidized surfaces.

"Inconel" 600

As found by other investigators for a number of alloys,[9,14] the same two-layered scale was present on all five samples examined (1000, 5000, and 10,000 hr at 1000°C; 500 and 3000 hr at 1150°C). The outer layer was a spinel with the approximate composition of $(Co, Ni, Fe)(Cr, Mn)_2O_4$. The inner layer was essentially Cr_2O_3. The lattice parameters of either compound did not change significantly with oxidizing conditions.

In the alloy depletion zone, the manganese and chromium concentrations decreased, while the nickel and iron concentrations increased. The thickness of this zone measured on the microprobe scans agreed well with the thickness measured metallographically.

"Hastelloy" C

The scale was the same as found on "Inconel" 600: an outer layer of manganese-rich spinel and an inner layer of Cr_2O_3 (Fig. 7). Immediately below the scale was a band of globular oxide particles rich in silicon and tungsten with none of the other elements present. These particles could be easily mistaken for voids during metallographic examination because of their dark gray color. There was no molybdenum in any portion of the oxide.

The alloy depletion zone was not as well defined as in other alloys; the distinguishing metallographic characteristic was a change in the morphology of the particles in the matrix. The chromium and manganese concentrations decreased, the iron and molybdenum contents increased slightly, and the nickel, silicon, and tungsten concentrations were unchanged.

The particles in the matrix were identified as the "mu phase" that has been found in Ni–Co–Mo alloys[15] and in "Hastelloy" X.[8] The appropriate composition was $(NiCrFe)_7(MoWSi)_6$.

"Hastelloy" X

The compositions of the scale and the underlying zone of globular particles were the same as on "Hastelloy" C, except that no tungsten was
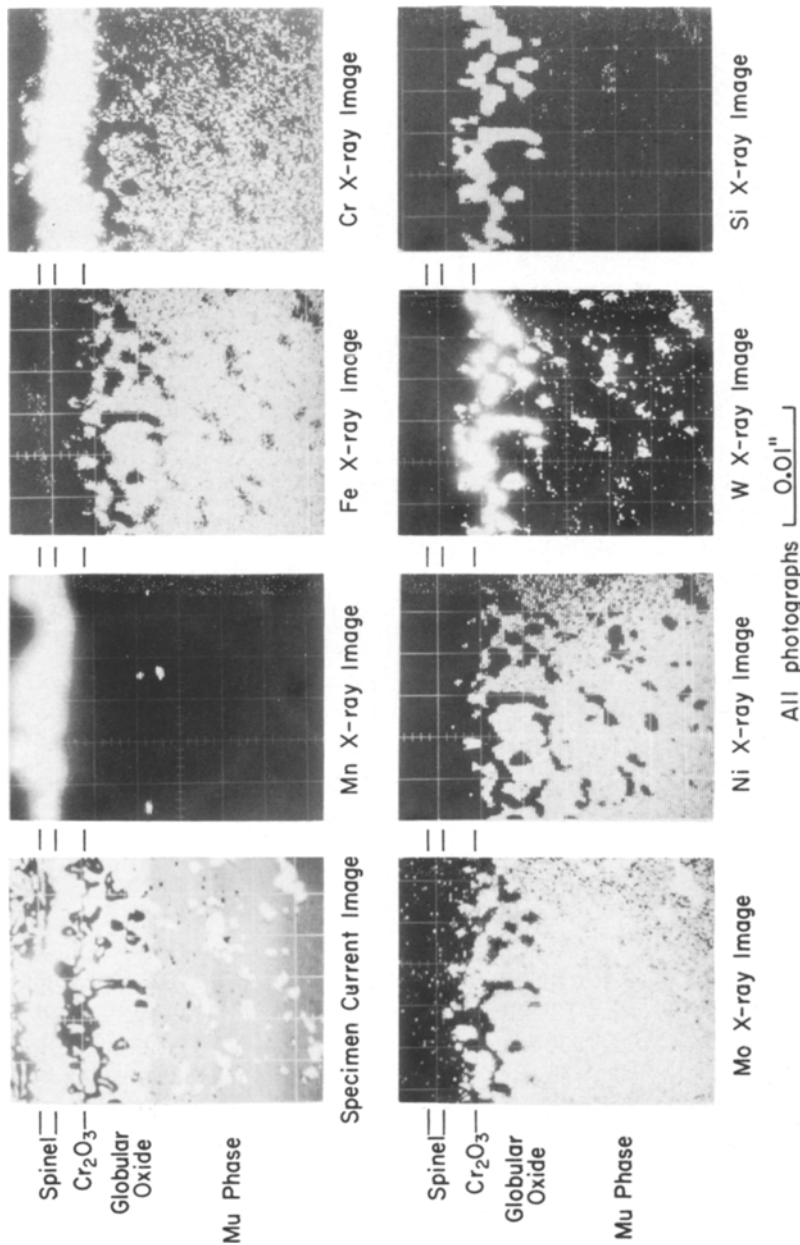
Fig. 7. Composition of oxidation-affected zone in "Hastelloy" C after 10,000 hr at 1000°C. The presence of spinel in the outer layer of the oxide scale is indicated by the Mn, Fe, and Cr images; Cr_2O_3 in the inner layer is indicated by the Cr image and the absence of other elements in the corresponding region. The subsurface particles are rich in W and Si, and the particles in the matrix are rich in Mo with W and Si also present.

present (none present in this alloy initially). The mu phase was present in the matrix.

"Haynes" 25

The composition of the scale changed when the oxidation rate changed. Scales formed after 1000, 5000, and 10,000 hr at 1000°C and after 500 hr at 1150°C were the same as observed on the "Hastelloys," an outer layer of spinel, an inner layer of Cr_2O_3, and a zone of globular particles rich in tungsten and silicon. In the alloy depletion zone, the chromium, manganese, and silicon concentrations decreased, but the cobalt, nickel, iron, and tungsten concentrations increased.

The thick, multilayered scale formed during 3000 hr at 1150°C was a complex mixture of cobalt oxides, cobalt tungstate, spinel, and silicates (Fig. 5). The outer layer was predominantly CoO with Co_3O_4 precipitated along the surfaces of the cracks, at the grain boundaries, and within some of the grains. The other alloying elements were present in solution in minor amounts. The five inner layers were composed of a nearly homogeneous mixture of spinel and $CoWO_4$ with $(Co, Fe)_2SiO_4$ concentrated in alternate layers (layers 3 and 5).

Although the manner in which this thick scale is formed cannot be explained at present, the presence of the tungstate, as also observed by Wlodek[10] and Wolf and Sandrock,[11] suggests a causal relationship. For example, the rapid oxidation may be associated with the decomposition of the tungstate to form WO_3 vapor and the outer layer of CoO. However, Douglass and Armijo[16] observed a scale with similar appearance in Co–Cr–Mn and Co–Cr–Si alloys.

EFFECT OF ALLOY COMPOSITION ON OXIDATION RESISTANCE

Differences in oxidation resistance among the four groups of alloys (Table I) can be attributed qualitatively to the effects of certain alloying elements. These effects are illustrated by the curves shown in Fig. 8 that were obtained by the technique of graphical multiple correlation.[17] The parameters used in this analysis were the nominal composition and the expected total depth affected by oxidation at 1000°C after 50,000 hr. Four iterations of the analysis were required to eliminate further effects on the shapes of the curves.

Chromium

The well-known increase in oxidation resistance[9,18] provided by chromium additions of .15 to 20 wt.% was again demonstrated by these
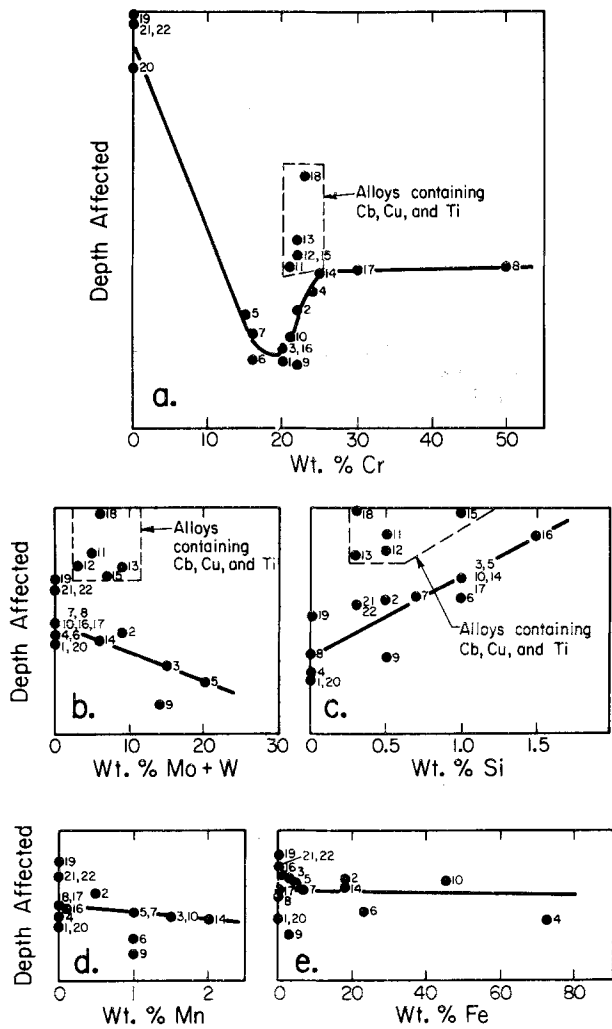
Fig. 8. Effect of alloy content on depth affected by oxidation at 1000°C. Numbers beside data points refer to alloys listed in Table I. Vertical axes drawn to same scale. Curves show trends for indicated range of compositions and should not be extrapolated to higher concentrations.

tests [Fig. 8(a)]. The majority of the more oxidation-resistant alloys of groups A and B have chromium contents within this range. In contrast, the alloys of group D contain no chromium, and the alloys of group C contain > 20 wt.% chromium.

Molybdenum and Tungsten

Increasing the molybdenum and tungsten contents increased the resistance to oxidation [Fig. 8(b)]. The more resistant alloys of group B, "Hastelloy" X, "Haynes" 25, and "Hastelloy" C, have the highest molybdenum and tungsten contents. The beneficial effect of tungsten may only apply at 1000°C. The rapid oxidation of "Haynes" 25 at 1150°C may be associated with tungsten, as discussed above.

Silicon

Increasing silicon contents lower the resistance to oxidation [Fig. 8(c)]. For example, "Tophet" A is less resistant than "Inconel" 600, although the compositions are similar except for the higher silicon content of "Tophet" A.

Columbium, Copper, and Titanium

Columbium, copper, and titanium apparently reduce the resistance to oxidation [data points for alloys containing these elements always lay above the curves, Figs. 8(a) through 8(c)]. Several alloys in group C contain up to 4 wt.% of these elements; these levels counteract the beneficial effects of the intermediate levels of tungsten and molybdenum that are also present in these alloys. For example, "Inconel" 625, with a composition similar to that of "Hastelloy" X, except for the addition of 4 wt.% columbium, is significantly less resistant to oxidation than is "Hastelloy" X. The detrimental effects of columbium and titanium have been reported previously.[9] Titanium increases the susceptibility to intergranular penetration, as shown in these tests by "Incoloy" 825, which had deeper intergranular attack than any of the other alloys tested.

Manganese

Manganese has only slight, if any, beneficial effect, on oxidation resistance [Fig. 8(d)]. Some beneficial effect might be expected because manganese is a principal constituent of the spinel oxide that forms during parabolic oxidation.

Iron

Iron has no effect on oxidation resistance, as might be expected, because its properties are similar to nickel and cobalt [Fig. 8(e)].

Lanthanum and Yttrium

The reported increase in oxidation resistance provided by additions of rare-earth elements was not confirmed conclusively by these tests.[19] "Haynes" 188, containing 0.5 wt.% lanthanum, was more resistant than expected for the given levels of the other alloying constituents (data point lies below the curves in Fig. 8). However, "Haynes" 188 was less resistant than "Haynes" 25, an alloy of a similar composition with no lanthanum added. GE 2541, containing 0.2 wt.% yttrium and 4 wt.% aluminum, was no more resistant than expected for its particular iron and chromium contents. A similar Fe–Cr–Al alloy with no yttrium was reported to be more resistant than GE 1541 in 600-hr tests at up to 1093°C.[7]

Thorium Oxide

TD Nickel chromium, containing 2 wt.% ThO_2, was more resistant to oxidation than any of the alloys tested, indicating a large beneficial effect. This is exemplified by the greater resistance of TD nickel chromium compared to "Tophet" A; both are essentially 80Ni–20Cr alloys, but TD nickel chromium contains 2% ThO_2 added. In contrast, a similar addition of ThO_2 to pure nickel had no effect on oxidation resistance.

ACKNOWLEDGMENT

The author gratefully acknowledges the work of A. E. Symonds in performing the microprobe analyses and assisting in the oxidation testing.

REFERENCES

1. C. P. Ross, *Isotop. Rad. Tech.* **5**, 185 (1968).
2. C. P. Ross, C. L. Angerman, and F. D. R. King, USAEC Report DP-1096, Savannah River Laboratory (1967).
3. C. L. Angerman, F. D. R. King, J. P. Faraci, and A. E. Symonds, *Nuclear Appl.* **4**, 88 (1968).
4. C. L. Angerman and J. P. Faraci, *Nuclear Metal.* **14**, 309 (1969).
5. C. L. Angerman and C. P. Ross, "Performance of ^{60}Co Capsules at Heat Source Conditions" presented at Fifth Annual Inter-society Energy Conversion Engineering Conference, Las Vegas, Nevada, September 21–25, 1970 (to be published).
6. S. T. Wlodek, *Trans. AIME* **230**, 177 (1964).
7. F. W. Cole, J. B. Padden, and A. R. Spencer, NASA Report NASA-CR-930, Bendix Corp. (1968).
8. W. L. Clarke, Jr., and G. W. Titus, USAEC Report AGN-8289, Vol. I, Aerojet-General Corp. (1968).
9. C. H. Lund and H. J. Wagner, Defense Metals Information Center Report DMIC-214, Battelle Memorial Institute (1965).
10. S. T. Wlodek, USAEC Report R64FPD12, General Electric Co. (1964).

11. J. S. Wolf and G. D. Sandrock, NASA Report NASA-TN-D-4715, Lewis Research Center (1968).
12. G. R. Wallwork and A. Z. Hed, *Oxid. Metals* **3**, 229 (1971).
13. H. H. Davis, H. C. Graham, and I. A. Kvernes, *Oxid. Metals* **3**, 431 (1971).
14. S. J. Grisaffe and C. E. Lowell, NASA Report NASA TN D-50-A, Lewis Research Center (1969).
15. D. K. Das, S. P. Rideout, and P. A. Beck, *Trans. AIME* **194**, 1071 (1952).
16. D. L. Douglass and J. S. Armijo, *Oxid. Metals* **3**, 185 (1971).
17. O. B. Ellis, *Corrosion* **9**, 203 (1953).
18. W. A. Rentz and M. J. Donachie, Jr., American Society for Metals Technical Report C6-18.5 (1966).
19. F. R. Morral, *Corrosion* **25**, 307 (1969).
20. H. E. Collins, *Trans. ASM* **62**, 82 (1969).